Expert Systems with Applications 39 (2012) 7132–7137

Contents lists available at SciVerse ScienceDirect

Expert Systems with Applications

journal homepage: www.elsevier.com/locate/eswa

Applications of thermal image and extension theory to biometric personal recognition

Meng-Hui Wang *, Yu-Kuo Chung

Department of Electrical Engineering, National Chin-Yi University of Technology, Taiwan

ARTICLE INFO

Keywords:
Thermal image
Extension method
Personal recognition system

ABSTRACT

In this paper, a new scheme is proposed to design a biometric personal recognition system. First, this paper used the thermal image of the hand by using infrared camera to build the sensor module of the recognition system; the extraction features include the length of palmar midpoint to each finger, palmar profile, finger length and finger width. The thermal image presented in this paper was detects infrared energy and converts it into an electronic signal. Then a new recognition method based on the extension is proposed to perform the core of the personal recognition system. The experimental results confirmed that proposed recognition system has a very high recognition rates, therefore, this paper verification using thermal image of the hand to identity recognition was feasible.

1. Introduction

The biometric authentication technology is a new method for recognizing the identity of a person based on an already established database of physiological or behavioral characteristics (Su, 2008; Teng, Wu, Yu, & Liu, 2005; Zhang, 2000). These physiological characteristics are unique, invariant, carry-on and permanent (Chang, Tsai, & Yu, 2008; Horio & Yamakawa, 2007), cannot be imitated and are carried with the individual without remembering. Furthermore, each kind of biometric identification technique has a relevant reference literature, such as the fingerprints (Jain, Hong, Pankanti, & Bolle, 1997), hand shapes (Reillo, Avila, & Marcos, 2000), palm prints (Savic & Pavesic, 2007; Zhang, Kong, You, & Wong, 2003), facial characteristics (Karungaru, Fukumi, & Akamatsu, 2007) and iris. The recognition system based on physiological characteristics has high accuracy. The development of biometric authentication technology can solve the problems of the traditional security method, and presently, this technique has the trend of replacing the traditional verification method. Most biometric authentication technologies aim at the hand characteristics, due to the diversified characteristics of palms. When capturing the hand images, the surrounding environment and lighting can affect the quality of hand images, causing wrong identifications when poor images have been acquired. The earlier hand identification systems employed CCD cameras and have the following disadvantages: (1) CCD only produces images in the daytime and cannot be used in the dark. A lighting device must be installed to solve this problem; (2) when the traditional CCD identifies the hand shape characteristics, errors may occur and identification rate may be lowered due to different lengths of fingernails, dirt or wound during feature extraction.

Thermal images can be used to improve the above CCD hand identification system: (1) without the problem of light interference, photographs can be taken under inadequate lighting; (2) thermal images can detect the radiation heat emanated from human bodies; hence, it is not affected by different lengths of fingernails, dirt or wounds, and does not lead to errors and lower the identification rate; (3) the thermal imaging is a non-contact and noninvasive image capture method that can avoid causing any uncomfortable feelings of users. Therefore, this paper presents the thermal imaging method to capture hand characteristics, where the hand shapes are regarded as the characteristics for the identification without the effect of lighting or the ambient environment, and the extension method is used to recognize individual hands.

2. The proposed recognition system

2.1. The structure of the thermal image system

The structure of the proposed palmar recognition system is shown in Fig. 1. The hand recognition is performed on thermal image of the palmar surface acquired by an infrared thermal imaging camera. Thermal imaging detects the infrared wave signals of radiation. (See Fig. 2).

2.2. The acquired method of the palmar thermal images

The first step of the palmar recognition must acquire the interested zone or plamar shape of a thermal image. It is necessary to

* Corresponding author. Tel.: +886 4 23954505 2200; fax: +886 4 23924419.
E-mail address: wangmh@ncut.edu.tw (M.-H. Wang).

0957-4174/$ - see front matter © 2012 Elsevier Ltd. All rights reserved.
doi:10.1016/j.eswa.2012.01.031

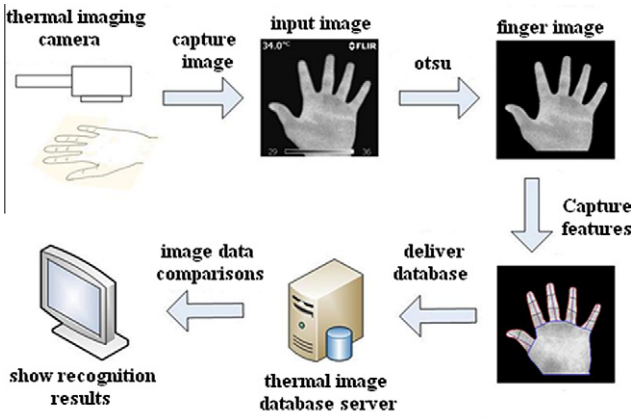

Fig. 1. The structure of the proposed palmar recognition system heat of the objects using the photoelectric infrared thermal imaging camera and transforms points into images (Wang, Leedham, & Cho, 2008), based on this, the temperature of detected objects can be known. In this study, a suitable shooting device was designed, as shown in Fig. 2. The device is consisted of aluminum alloy and features light weight and greater specific heat. The aluminum alloy temperate does not vary due to hand touch, so the aluminum alloy temperature is lower than the temperature of hand. Since the thermal imaging analyzers do not detect it, the aluminum alloy part is captured by the thermal imaging system. Then a preprocessing module is used for enhancing the geometric image of palmar surface, and a feature extraction module is used to compute the geometric parameters based on the processed image. The matching module compares the input's model with the stored typical models in the database to generate the relational degrees, a new recognition method based on the extension theory will be proposed in this paper. The final recognition results can be taken by the decision module according relational degrees.

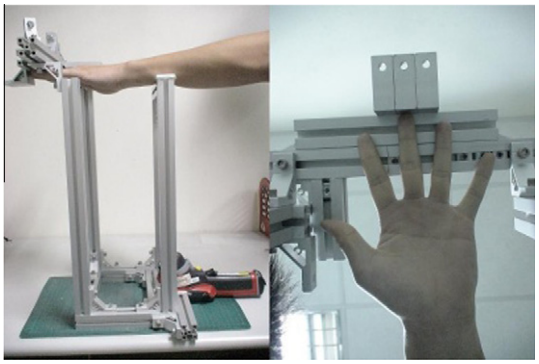

Fig. 2. The acquired device of the thermal image of palmar surface.

separate the palm on the thermal image from the background, where the background, noise and words of the thermal image are expressed by the gray value 0 (black). In this paper, using Otsu's method (Otsu, 1979) involves iterating through all the possible threshold values and calculating a measure of spread for the gray level threshold values. This technique applies the principle of statistics method for identification and analysis to obtain the optimal gray level threshold. Assuming the range of the image grey level value is $[1,R]$, the number of pixel points of the grey level value is i where $i \in [1,R]$, the accumulated number of points of each grey level is $n_1, n_2, \ldots, n_R$, the total number of points is T, and the probability distribution of the grey level I is expressed by Eq. (1).

$$P_i = \frac{n_i}{T}, \quad P_i \geqslant 0, \quad \sum_{i=R}^{R} P_i = 1 \tag{1}$$

The threshold value t is used to divide the image pixel into two clusters, C_a and C_b. C_a denotes the pixel cluster of the gray level range $[1,t]$; C_b denotes the pixel cluster of the gray level range $[t+1,R]$. The probability distribution of the two clusters is W_a and W_b, respectively, and the average values of the two clusters are μ_a and μ_b, then:

(a) Original image (b) Image separated from background

Fig. 3. Using Otsu's method to separate palm from background.

$$W_a = \sum_{i=1}^{t} P_i = W(t) \tag{2}$$

$$W_b = \sum_{i=t+1}^{R} P_i = 1 - W(t) \tag{3}$$

$$\mu_a = \sum_{i=1}^{t} \frac{iP_i}{W_a} = \frac{\mu(t)}{W(t)} \tag{4}$$

$$u_b = \sum_{i=t+1}^{R} \frac{iP_i}{W_b} = \frac{u_T - u(t)}{1 - W(t)} \tag{5}$$

The variances of these two clusters are σ and σ, the total variance is σ, then:

$$\sigma_a^2 = \sum_{i=1}^{t} (i - u_a)^2 \frac{p_i}{w_a} \tag{6}$$

$$\sigma_b^2 = \sum_{i=t+1}^{R} (i - u_b)^2 \frac{p_i}{w_b} \tag{7}$$

$$\sigma_w^2(t) = w_a\sigma_a^2(t) + w_b\sigma_b^2(t) \tag{8}$$

If the t value with a minimum total variance σ can be found, t is the optimal grey level threshold value. If the grey level of the image pixel is greater than the t value, the grey level is not changed; if it is smaller than the t value, it is set as 0. By using Eq. (9), the grey level is reassigned back to the image to separate the hand from the background and image brand. Fig. 3 shows the difference between the original image and the image treated by Otsu.

$$\text{Gray}(i,j) = \begin{cases} 0 & \text{if Gray}(i,j) < t \\ \text{Gray}(i,j) & \text{if Gray}(i,j) \geqslant t \end{cases} \tag{9}$$

2.3. Detecting palmar edge

Before capturing the palmar shape characteristics, the action of detecting the palmar edge must be made. The coordinates of palmar edge location can be found through Fig. 3. The edge can be detected by scanning the pixel points, where the scanning is divided into two stages. At stage 1, the images are scanned vertically from top to bottom, and the pixel points move from the left to the right. If the left and right adjacent gray values of the pixel points are all greater than 0, the location of the pixel coordinates are memorized and expressed by white points. However, some places are missed in detection. Hence, at stage 2, the images are scanned from the left to the right in the horizontal direction, and the pixel points move

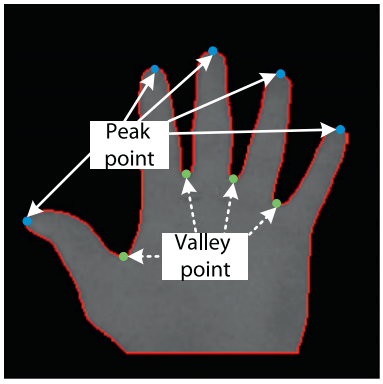

Fig. 4. Coordinates of valley points and peak points.

from top to bottom. If the upper and adjacent gray values of the pixel points are all greater than 0, the location of the pixel coordinates are also memorized. After the scanning action of the two stages, the palm edge coordinates can be detected thoroughly.

The palm edge coordinates contain the valley points and peak points of fingers; in Fig. 4, the points corresponding to solid lines are the coordinates of peak points, and the points corresponding to white dotted lines are the coordinates of valley points. In this paper, the valley and peak points are defined by calculating the Euclidean Distance between some point i in the coordinate set S_b of the palm edge and the starting point of the palm contour S_1, as shown in Fig. 5. Eq. (10) is used to calculate the Euclidean Distance, where D_i is the distance value between each coordinate and the starting point c. The i represents the sequence of coordinate contour; X_i and Y_i are the coordinate values of each coordinate contour; and X_c and Y_c are the coordinate values of the starting point.

$$D_i = \sqrt{(X_i - X_c)^2 + (Y_i - Y_c)^2}, \quad i \in S_b \tag{10}$$

In the clockwise direction, the palm contour coordinates S_b starts from the starting point c and returns to the starting point c. Eq. (10) is used to calculate the distribution of distance between c and each coordinate on the palmer contour, as shown in Fig. 6.

The distance distribution in Fig. 6 illustrates the five filled circles of peak points and the four slash circles of valley points, where the indicated coordinates are exactly the peak and valley points in Fig. 4. In this paper, another three valley points must be found to extract the features of the length and width of five fingers. In Fig. 7, white solid lines represent the left valley points of the thumb and the index finger, and the right valley point of the little figure. The point-increase method is to utilize the distance between the coordinates of a known valley point and a known peak point to find the coordinate point with the same distance on the opposite side. As shown in Fig. 9, after calculating the distance between the known coordinates of P and V points, the N point coordinate can be found by adding the $P - V$ distance from P point on the opposite side of V point, where N point is a new valley point. This method can help to find all three new valley points.

2.4. Feature extraction method

For the feature extraction of palmar shapes, there are a total of 34 features, which become fixed features after reaching a certain age of the peoples, hence, they can be used as recognition features. The proposed features in this paper are summarized in Table 1. The palmar contour size of each person is different; therefore, the number of palmar edge pixel points can be regarded as the identification feature after calculation, as well as the palmar contour after

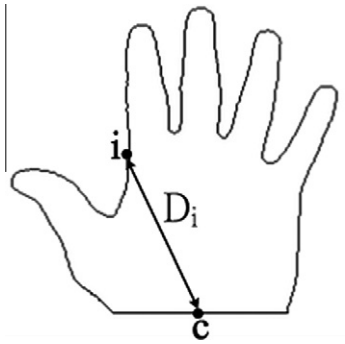

Fig. 5. Distance between contour and point c.

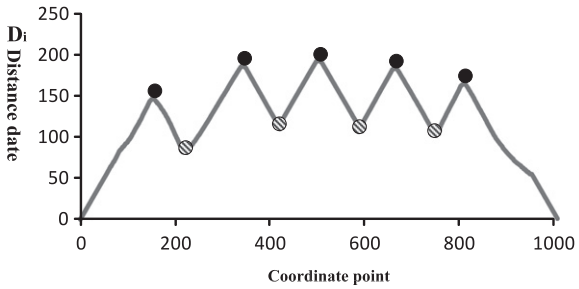

Fig. 6. Distribution condition of the distance between palmar contour coordinates and point c.

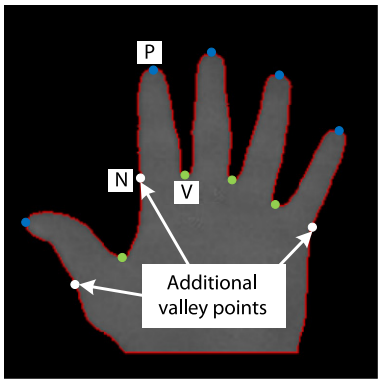

Fig. 7. Additional valley points.

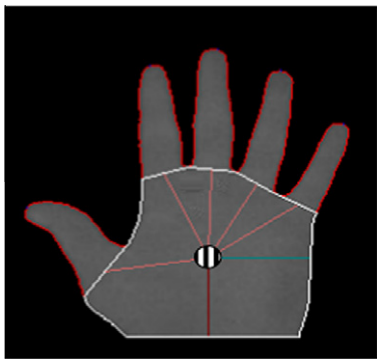

Fig. 8. Feature of palm distance distribution.

excluding the fingers (Otsu, 1979). The next step is to find the gravity point of palm images, where the distance from that point to the palm contour and the distances from that point to the fingers, are

Table 1
Palm shape feature.

C1	Hand contour	C18	1/3 width of index finger
C2	Palm contour	C19	2/3 width of index finger
C3	Horizontal distance of gravity	C20	Contour of middle finger
C4	Vertical distance of gravity	C21	Length of middle finger
C5	Distance between gravity and thumb	C22	Width of middle finger
C6	Distance between gravity and index finger	C23	1/3 width of middle finger
C7	Distance between gravity and middle finger	C24	2/3 width of middle finger
C8	Distance between gravity and third finger	C25	Contour of third finger
C9	Distance between gravity and little finger	C26	Length of third finger
C10	Contour of thumb	C27	Width of third finger
C11	Thumb length	C28	1/3 of width of third finger
C12	Thumb width	C29	2/3 of width of third finger
C13	1/3 width of thumb	C30	Contour of little finger
C14	2/3 width of thumb	C31	Length of little finger
C15	Contour of index finger	C32	Width of little finger
C16	Length of index finger	C33	1/3 of width of little finger
C17	Width of index finger	C34	2/3 width of little finger

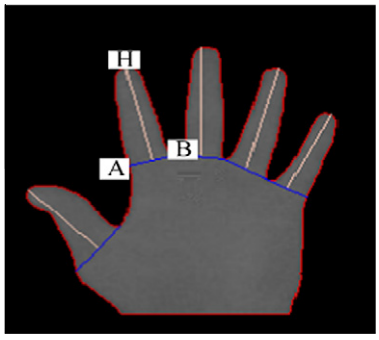

Fig. 9. Finger length feature.

being used as identification features. The gravity point coordinate can be determined by Eq. (11) where the C_x and C_y is the center coordinates of the image, H is the Heaviside step function and is only equal to 1 when $\varphi > 0$, otherwise, it is 0. The denominator represents the number of total pixel points within the palm contour, and the numerator represents the summation of x and y coordinates within the palm contour. After averaging, the gravity coordinate can be determined and is shown as white solid line circles in Fig. 8.

$$C_x = \frac{\sum_x \sum_y x \cdot H(\varphi)}{\sum_x \sum_y H(\varphi)}, \quad C_y = \frac{\sum_x \sum_y y \cdot H(\varphi)}{\sum_x \sum_y H(\varphi)} \tag{11}$$

After the gravity coordinate is determined, the distribution features of palm gravity distances can be extracted, including the distance between the gravity coordinate and valley points of each fingers and the distance between the gravity coordinate and the midpoints of valley points, and the horizontal and vertical distances between the gravity coordinate and palm contour, as shown in Fig. 8. The finger length extraction method is to calculate the midpoint coordinate between points A and B, and the distance between the midpoint and the H point is the length of the finger, as shown in Fig. 9. Normally, people have five fingers, so there are five length features.

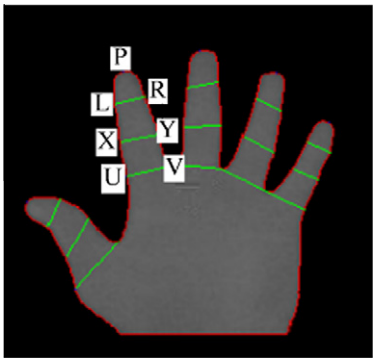

Fig. 10. Finger width feature.

Fig. 11. Finger size feature.

In addition, three widths of each finger are extracted and regarded as features. As shown in Fig. 10, the distance between U and V points is the first width of the index finger; the 2/3 distances between P and U points, and P and V points are coordinately labeled as points X and Y, the distance between them is the second width; the 1/3 distances between P and U points, and P and V points are labeled as points L and R of which the distance is the third width of the index finger. There are a total of 15 width features. The finger length and width features are not enough to represent the physiological features of a person and cannot determine the uniqueness of each individual. Only using these two features may result in incorrect identifications. The identification features which can represent the identity of a person should be increased and enhanced. This study extracted the finger sizes and regarded them as identification features. When determining the finger sizes, the contour coordinates of each finger should be found, and then the valley points and peak point of each finger can be connected, as shown in Fig. 11. At this time, each finger can form its own independent closed curve. Meanwhile, the number of white pixel points is the feature of the finger size.

3. The proposed pattern recognition method

At the recognition stage the inputting patterns are compared with the patterns stored in the system database. Learning from a set of training pattern is an important feature of most pattern recognition systems. The neural networks are usually used for pattern recognition, the advantage of a neural network over other classifiers is that it can acquire experience from the training data, but the training data must be sufficient and compatible to ensure proper training, its convergence of learning is influenced by the network topology and values of learning parameters. To overcome the limitations of the MNN mentioned, a new pattern recognition method,

based on the extension theory, is presented for palmer recognition in this paper.

3.1. Outline of extension theory

Extension theory is a new kind of knowledge system based on the concepts of matter-elements and extension sets. It was first proposed by Cai to solve contradictions and incompatibility problems in 1983 (Kumar, Wong, Shen, & Jain, 2006). Extension theory (Wang, 2005, 2006) consists of two parts, matter-element model and extended set theory. With the combination of extension theory and management science, cybernetics, information science and computer science, extension-engineering methods have been applied to some engineering fields such as economic engineering, management engineering, decision processes and process control (Styvaktakis, 2007; Wang, 2003).

3.2. The proposed recognition algorithm

In this paper, the proposed recognition method is based on the extension theory; it is The first step is to formulate matter-element models of hand types, and then hand types of tested hand can directly be identified by the degree of extended correlation function. The proposed recognition algorithm is described as follows:

Step 1: Formulating the matter-element of every typical palmar type as follows:

$$R_i = (H_i, C_i, V_i) = \begin{Bmatrix} H_i, & c_i, & \langle a_{i1}, b_{i1}\rangle \\ & \vdots & \vdots \\ & c_{34} & \langle a_{i34}, b_{i34}\rangle \end{Bmatrix} \quad \text{for } i = 1, 2, \ldots, P \tag{12}$$

where

H_i: the ith hand pattern P: the number of the palmar patterns c_j: the c_j: the jth feature.

a_{ij}: the low-bounds value of classical domains in the jth feature for ith palmar pattern.

b_{ij}: the up-bounds value of classical domains in the jth feature for ith palmar pattern.The ranges of classical domains $V = \langle a, b\rangle$ of every feature can be directly obtained from the low-bounds and up-bounds of training patterns, or determined from previous experience.

Step 2: Input a palmar pattern of tested person; and formulating the matter-element of this tested pattern as follows:

$$R_t = (H_t, C_t, V_t) = \begin{Bmatrix} H_t, & c_1 & v_{t1} \\ & \vdots & \vdots \\ & c_{34} & v_{t34} \end{Bmatrix} \tag{13}$$

where $v_{t1}, v_{t2}, \ldots, v_{t34}$ are the values of tested pattern.

Step 3: Calculating the degrees of correlation of the tested pattern with the characteristic of the typical patterns by the proposed extended correlation function as follows:

$$K_{ij}(v_{tj}) = \begin{Bmatrix} \frac{-2\rho(v_{tj}, V_{ij})}{|b_{ij} - a_{ij}|}, & \text{if } v_{tj} \in V \\ \frac{\rho(v_{tj}, V_{ij})}{\rho(v_{tj}, \hat{V}_{ij}) - \rho(v_{tj}, V_{ij})}, & \text{if } v_{tj} \notin V_{ij} \end{Bmatrix}, \quad i = 1, 2, \ldots, P; \quad j = 1, 2, \ldots, 34 \tag{14}$$

where

$$V_{ij} = \langle a_{ij}, b_{ij}\rangle \tag{15}$$

$$\hat{V}_{ij} = \langle f_{ij}, g_{ij}\rangle \tag{16}$$

The neighborhood domain $\hat{V} = \langle f, g\rangle$ of classical domains, the possible range values of every characteristic can be determined. They are set as $f = 0.95 \times a$ and $g = 1.05 \times b$ in this paper. The proposed extended correlation function can be shown as Fig. 12, where $0 \leqq K(v) \leqq 1$ corresponds to the normal fuzzy set. It describes the degree to which v belong to V. When $K(v) < 0$, it indicates the degree to which v does not belong to V, which is not defined in the fuzzy theory and is a main advantage of the extension theory.

Step 4: Setting the weights of every degree of correlation, $w_1, w_2, \ldots, w_{34}$, depending on the importance of every feature in the recognition process. In this paper, all weights are set at 1/34.

Step 5: Calculating the indexes of correlation for every palmar type as Eq. (17). Generally, the high correlation index implies that the tested palmar pattern has the high probable to belong to this palmar type.

$$\beta_i = \sum_{j=1}^{34} w_j K_{ij}, \quad i = 1, 2, \ldots, \mathrm{p} \tag{17}$$

Step 6: Ranking all correlation indexes to find the maximum correlation index as following:

$$\beta_{\max} = \max_{1 \leqslant i \leqslant p} \{\beta_i\} \tag{18}$$

Step 7: The recognition rule is shown as follows:

If $(\beta_{\max} = \beta_k)$ AND $(\beta_k \geqq \delta)$ THEN (the tested palmar pattern belong to kth palmar type) where δ is the optimal threshold value, it set to 0.474 in this paper, the optimal threshold value can be calculated when the False Rejection Rate (FRR) equals False Acceptance Rate (FAR), the detail can be shown in Fig. 13. Assuming the false rejected sample is N_r, the false accepted sample is N_a, and the total testing sample is N_t, the FRR and FAR can be circulated by Eqs. (19) and (20).

$$FRR = \frac{N_r}{N_t} \tag{19}$$

$$FAR = \frac{N_a}{N_t} \tag{20}$$

Step 8: Going back to step 2 for the next tested hand when the recognition of one has been completed, until all have been done.

The main advantage of the proposed method is that it can provide more detailed information about matched probability of the tested palmar pattern with stored patterns by indexes of correlation. Moreover, the proposed method does not need to spend learning time or to tune weights, and a simple software package can easily implement it for portable tools.

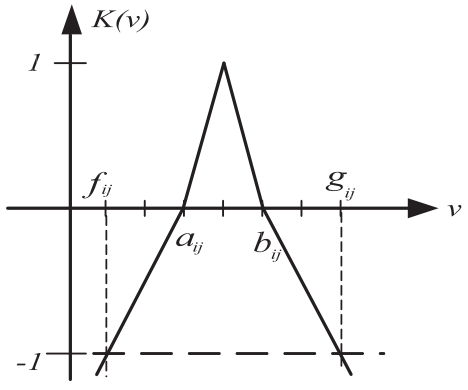

Fig. 12. The proposed extended correlation function.

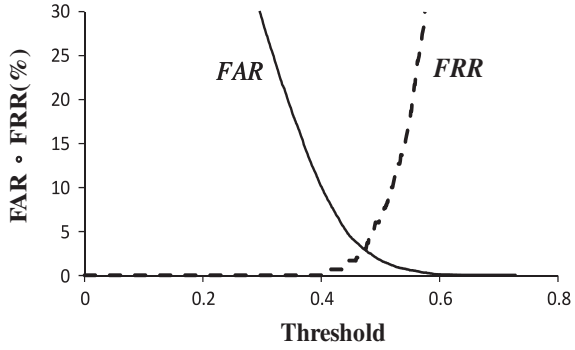

Fig. 13. The found method of optimal threshold value.

Table 2
Recognition performances of different methods.

Recognition methods	Learning times	Learning accuracy (%)	Testing accuracy (%)
Proposed method	0	93	92
K-means clustering	0	70	68
Neural network(34-33-30)	1000	91	88
Neural network(34-34-30)	1000	93	90

4. Experimental results

The tested samples were 300 images with 30 persons, and 10 images each. The optimal element model or neural weight value of neural networks was found through data training. The training characteristics of the four recognition algorithms are summarized in the Table 2. The accuracy of traditional recognition method was compared with the proposed method. As seen, the proposed method has the best recognition effect where the learning accuracy and testing accuracy. The proposed method in both the learning and testing accuracy has a significantly higher diagnosis accuracy of 93% and 92%, respectively, which are higher than other the other identification methods.

5. Conclusions

This study applied a thermal imaging camera to capture the palmar images to develop the person's recognition system. First, the images were pre-treated; then, the palm contour was detected to extract the features. The images were not affected by the lighting, and the hand position was not fixed when shooting by a thermal imaging camera. The users simply had to open their hands for the shooting. Furthermore, the accuracy of the proposed recognition algorithms was higher than the traditional recognition algorithm. The recognition system was designed for the hand geometric features only; if it could be combed with other recognition systems, such as the face, iris, and finger, the security could be increased.

References

Chang, B., Tsai, H., & Yu, P. (2008). Handwritten character recognition using neuro-fuzzy system. *International Journal of Innovational Computing and Information Control, 4*(9), 2345–2362.

Su, C.-L (2008). Hand image recognition by the techniques of hand shape scaling and image weight scaling. *Expert Systems with Applications, 34*, 2976–2987.

Horio, K., & Yamakawa, T. (2007). Handwritten character recognition based on relative position of local features extracted by self-organizing maps. *International Journal of Innovational Computing and Information Control, 3*(4), 789–798.

Jain, A. K., Hong, L., Pankanti, S., & Bolle, R. (1997). An identity authentication system using fingerprints. *IEEE Proceedings, 85*(9), 1365–1388.

Karungaru, S., Fukumi, M., & Akamatsu, N. (2007). Automatic human faces morphing using genetic algorithms based control points selection. *International Journal of Innovational Computing and Information Control, 3*(2), 247–256.

Kumar, A., Wong, D. C. M., Shen, H. C., & Jain, A. K. (2006). Personal authentication using hand images. *Pattern Recognition Letters, 27*(13), 1478–1486.

Wang, L., Leedham, G., & Cho, D. S.-Y. (2008). Minutiae feature analysis for infrared hand vein pattern biometrics. *Pattern Recognition, 41*, 920–929.

Otsu, N. (1979). A threshold selection method from gray-level histograms. *IEEE Transactions on System, Man and Cybernetics, SMC-9*(1), 62–67.

Reillo, R. S., Avila, C. S., & Marcos, A. G. (2000). Biometric identification through hand geometry measurements. *IEEE Transactions on Pattern Analysis and Machine Intelligence, 22*(10), 1168–1171.

Savic, T., & Pavesic, N. (2007). Personal recognition based on an image of the palmar surface of the hand. *Pattern Recognition, 40*, 3152–3163.

Styvaktakis, E. (2007). Expert system for power quality disturbance classifier. *IEEE Transactions on Power Delivery, 22*(3), 1979–1989.

Teng, X., Wu, B., Yu, W., & Liu, C. (2005). A hand gesture recognition system based on local linear embedding. *Journal of Visual Languages and Computing, 16*, 442–454.

Wang, M. H. (2003). Extension neural network for power transformer incipient fault diagnosis. *IEE Proceedings Generation, Transmission and Distribution, 150*, 679–685.

Wang, M. H. (2005). Extension neural network – Type 3. *The Second International Symposium on Neural Networks, 3496*, 503–508.

Wang, M. H. (2006). Vibration fault diagnosis of large generator sets using extension neural network-type 1. In *Proceedings of the Third International Symposium on Neural Networks, ISNN 2006, Chengdu, China, Part II, May 28–June 1, 2006* (pp. 1395–1401).

Zhang, D. (2000). *Automated biometrics: technologies & systems*. Kluwer Academic.

Zhang, D., Kong, W. K., You, J., & Wong, M. (2003). Online palmprint identification. *IEEE Transactions on Pattern Analysis and Machine Intelligence, 25*(2), 1041–1050.